Stillwater Hybrid Geo-Solar Power Plant Optimization Analyses

Daniel S. Wendt[1], Gregory L. Mines[1], Craig S. Turchi[2], Guangdong Zhu[2], Sander Cohan[3], Lorenzo Angelini[3], Fabrizio Bizzarri[4], Daniele Consoli[4], and Alessio De Marzo[4]

[1]Idaho National Laboratory, Idaho Falls ID
[2]National Renewable Energy Laboratory, Golden CO
[3]Enel Green Power North America, Andover MA
[4]Enel Green Power — Innovation Div., Rome IT

Keywords

Hybrid geothermal solar thermal power plant, air-cooled binary cycle, organic Rankine cycle, ORC, concentrating solar power, simulation, optimization

ABSTRACT

The Stillwater Power Plant is the first hybrid plant in the world able to bring together a medium-enthalpy geothermal unit with solar thermal and solar photovoltaic systems. Solar field and power plant models have been developed to predict the performance of the Stillwater geothermal / solar-thermal hybrid power plant. The models have been validated using operational data from the Stillwater plant.

A preliminary effort to optimize performance of the Stillwater hybrid plant using optical characterization of the solar field has been completed. The Stillwater solar field optical characterization involved measurement of mirror reflectance, mirror slope error, and receiver position error. The measurements indicate that the solar field may generate 9% less energy than the design value if an appropriate tracking offset is not employed. A perfect tracking offset algorithm may be able to boost the solar field performance by about 15%.

The validated Stillwater hybrid plant models were used to evaluate hybrid plant operating strategies including turbine IGV position optimization, ACC fan speed and turbine IGV position optimization, turbine inlet entropy control using optimization of multiple process variables, and mixed working fluid substitution. The hybrid plant models predict that each of these operating strategies could increase net power generation relative to the baseline Stillwater hybrid plant operations.

Introduction

Geothermal energy is a reliable source for clean, renewable, base-load power. However, air-cooled geothermal power plants operate at reduced output levels during periods of elevated ambient temperature. Unfortunately, electrical power demand also tends to be greatest during periods at which ambient temperature is elevated, which results in power generation from air-cooled geothermal plants being out of sync with typical electrical load profiles.

Solar energy is also used for renewable power generation. Solar energy can be either directly converted to electrical power via photovoltaic devices or captured via concentrating solar thermal collectors such that the thermal energy output can be utilized by a thermoelectric power plant. In contrast to power generated from air-cooled geothermal plants, solar power is most plentiful during the time periods in which the electrical load is greatest. However, in the absence of thermal storage, solar power is unavailable at night or when the sun is obscured.

The aforementioned characteristics of geothermal and solar power generation create opportunities for synergistic use of these heat sources in a geothermal / solar-thermal hybrid power plant [1-12]. Geothermal / solar-thermal hybrid power plants have the ability to operate at higher output levels than comparably-equipped stand-alone air-cooled geothermal plants during periods when solar energy is available. Geo-solar hybrid plants don't require the heat storage infrastructure that would be required for a stand-alone solar plant to operate during periods when solar energy is unavailable. Additionally, a

single power block can be utilized to convert the geothermal and solar-thermal energy to electrical power rather than the two power blocks that would be required for two stand-alone geothermal and concentrated solar power plants.

The primary disadvantages associated with geo-solar hybrid plant technology are attributed to the relatively high capital costs for concentrating solar thermal collectors, and the inability of many power cycle configurations to effectively utilize heat supplied at different temperatures for efficient power generation. These challenges are currently being investigated via a Cooperative Research and Development Agreement (CRADA) partnership involving Enel Green Power (EGP), the National Renewable Energy Laboratory (NREL), and the Idaho National Laboratory (INL) with oversight from the U.S. Department of Energy Geothermal Technologies Office (GTO).

Figure 1. EGP Stillwater Geothermal/PV/CSP Plant Rendering.

EGP, NREL, INL and the GTO are working together to study the integration of geothermal and concentrated solar thermal heat sources for electrical power generation, with the goal of opening doors for the development of future hybrid renewable energy facilities. This paper describes CRADA tasks completed to date, including modeling the combination of geothermal and concentrating solar thermal systems, validating simulated results with real-world data from EGP's Stillwater hybrid facility, and using the validated models to quantify the potential benefits of different operating strategies.

The Enel Green Power Stillwater Hybrid Geothermal/Concentrating Solar Power (CSP) Project

Enel Green Power's Stillwater Geothermal/CSP project is the first hybrid plant in the world able to bring together at the same site the continuous generating capacity of binary-cycle, medium-enthalpy geothermal power with solar photovoltaic and solar thermal power.

Commencing operations during March 2015, the concentrating solar field adds an estimated 2MW of capacity (17MW thermal) to the existing 33MW Stillwater geothermal power plant. Production from the CSP plant will be integrated directly into the geothermal plant. It is the second solar facility on the site, joining a 26MW photovoltaic plant.

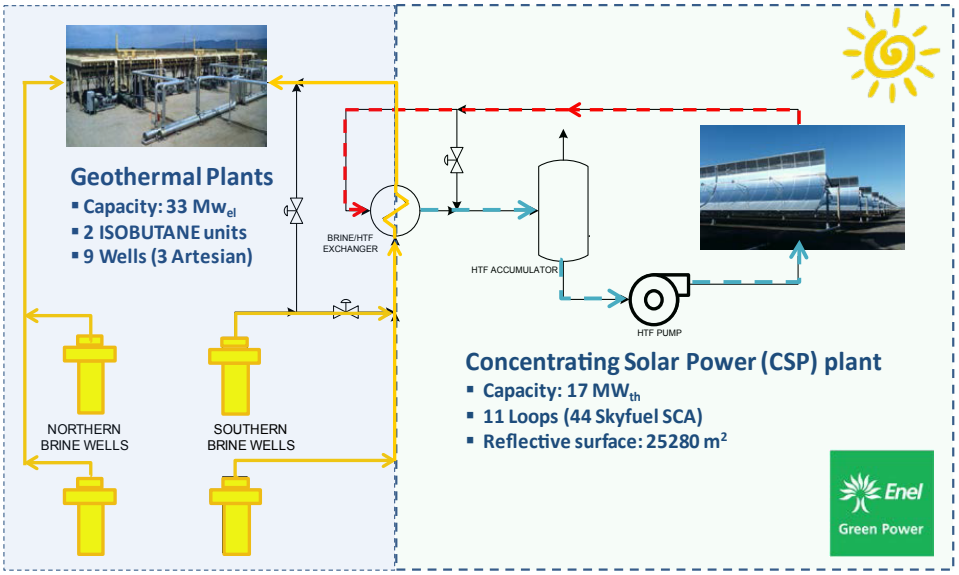

Figure 2. Stillwater CSP/GEO Process Flow Diagram Showing CSP Contribution to Geothermal Brine Temperature.

Figure 2 describes the main process of the project. The parabolic mirrors of the plant are used to direct solar energy to heat vacuum tubes filled with demineralized water. The heat collected by this system is then transferred to and augments the temperature of the geothermal fluid extracted from the facilities production wells, which is then used by the geothermal plant (via an Organic Rankine Cycle) to produce power.

The project consists of:

- 22 rows (11 loops) of parabolic solar concentrating mirrors; each row is 700 feet, each mirror is approximately 20 feet across, spread across more than 20 acres.

- Total of 2,772 mirror panels.
- Linear parabolic mirror totaling 24,778 m^2 (approx. 270,000 sq. ft.), capable of concentrating the solar radiation some 75 times, onto receiver tubes filled with demineralized water under pressure.

Enel Green Power embarked on this project as part of its ongoing Innovation efforts, specifically engaging in efforts to use hybrid applications to increase availability and mitigate intermittency seen in renewable energy projects.

As with the PV project before it the application of CSP is aimed at achieving these goals. The CSP plant is designed to improve the performance of the geothermal plant as a whole by providing an option of augmenting the input temperature of the geothermal plant with the heat of the sun, whose resource is more predictable and easily measurable. Specific anticipated benefits include:

- Increased production when the thermal efficiency of the geothermal unit is at its lowest.
- More delivery of power during peak hours, enabling a more load-following production profile.
- Less environmental footprint per unit of renewable energy produced and delivered.

In addition to near-term benefits of co-locating geothermal and CSP, the addition of CSP will allow for more effective management of the geothermal heat resource, which will potentially lead to lower long-term O&M costs.

Solar Field Characterization

Optical characterization of the solar field is critical to conduct the accurate prediction of solar field power output, which is essential for predicting how a combined geothermal/solar-thermal system will behave. A comprehensive optical test of the Stillwater plant's solar-thermal collector field was performed in December 2014. The optical testing measured the average solar field reflectance and the average solar collector optical error.

The solar field reflectance is obtained by using two portable reflectometer devices: Devices & Services R15 (D&S) [13] and Surface Optics Corporation Solar 410 (SOC) [14]. The former measures specular reflectance at varying acceptance aperture angles at a single wavelength of 660 nm and the latter measures solar-weighted specular reflectance at a large aperture angle. By combining measurements from two devices, solar weighted average reflectance including total specular reflectance and specularity can be derived.

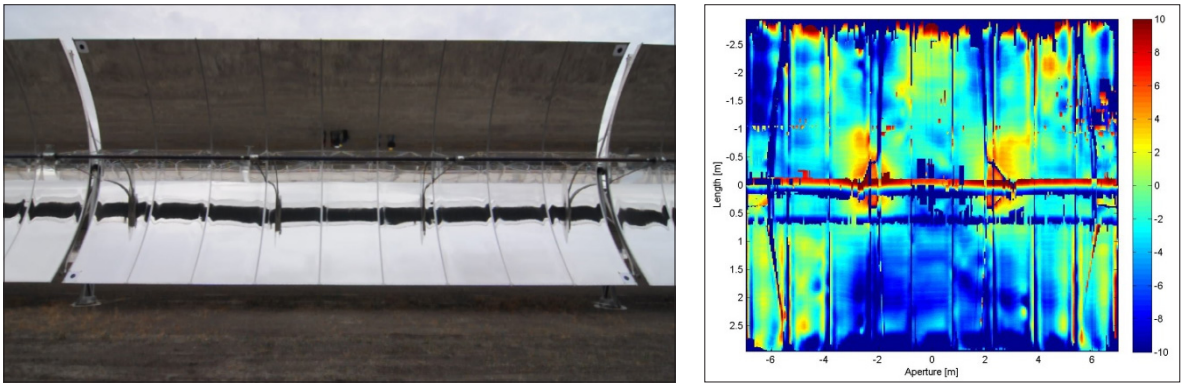

Figure 3. A snapshot of Distant Observer (DO) optical characterization: raw photo (left) and slope error map (right).

The collector optical error was characterized using NREL's Distant Observer (DO) methodology [15, 16]. DO is the first optical characterization tool in the world that can efficiently measure both the reflector slope error and the receiver position error at the same time in the field. DO simply requires a camera on a tripod to collect the reflection image. An example of a reflection image is shown in the left part of Figure 3. Then, an image-processing program is employed to analyze the images to derive mirror slope error. The right plot of Figure 3 shows an example of a mirror-slope error map, which accounts for both mirror slope error and receiver position error in this case.

The solar field at the Stillwater hybrid plant includes 11 loops of SkyTrough collectors, which con-

Table 1. Solar Collector Optical Specifications and Optical Error Measurements.

Parameter		Value	Source
Receiver	Absorptivity	0.96	Manufacturer
	Glass envelope transmissivity	0.97	Manufacturer
Mirror	Solar-weighted specular reflectance	0.904*	Measured
	Specularity RMS	1.915 mrad	Measured
	Slope error – mean value	-3.94 mrad	Measured, including the receiver position error.
	Slope error – mean value with tracking correction	1.00 mrad	
	Slope error – RMS	2.99 mrad	
Collector	Tracking error - RMS	1 mrad	Assumption

* measured average reflectance impacted by degradation to some panels that resulted from accidental water damage during storage

sists of a total 308 solar collector modules. Among all the modules, 44 modules were selected for reflectance measurements and 14 modules for DO measurements. After post-processing of the measurement data, the average optical measurement results were obtained, which are summarized in Table 1. The detailed results are reported elsewhere [17].

The overall solar field performance can be predicted from the optical test results using NREL's FirstOPTIC software [18] and System Advisor Model (SAM) [19]. An incident angle modifier (IAM) is typically used to describe the solar collector performance under non-zero incidence angle, that is, for different sun positions throughout the year. A common form for the IAM is:

$$IAM(\theta) = k_{IAM,0} + k_{\mathrm{IAM},1} \cdot \frac{\theta}{cos(\theta)} + k_{\mathrm{IAM},2} \cdot \frac{\theta^2}{cos(\theta)} + k_{\mathrm{IAM},3} \cdot \frac{\theta^3}{cos(\theta)} \quad (1)$$

The fitting function could be second-order or third-order. In general, the latter may provide less fitting error. SAM currently adopts the second-order IAM fitting function; however, an equation of this form was found to yield a poor fit to the Stillwater data. Accordingly, a third-order fit was applied and is shown in Figure 4.

The optical efficiency at a non-zero incidence angle is then:

$$\eta(\theta) = \eta_o \cdot IAM(\theta) = \rho\tau\alpha\gamma \cdot IAM(\theta) \quad (2)$$

Here, θ is the solar incidence angle in radians, ρ is the parabolic mirror reflectivity, τ the receiver glass envelope transmissivity, α the average receiver coating absorptivity, and γ the collector intercept factor. As measured, the predicted intercept factor is about 0.827 if no correction mechanism is used in the solar field. At the same time, it is observed that the total slope error has a mean value with a substantial magnitude, ranging from -2.9 mrad to -5.0 mrad. This indicates gravity-induce deflection of the receiver, which is most pronounced when the collectors are pointed at the horizon as they were for these measurements. In practice, this is compensated for by modification of the tracking algorithm. The slope error with a mean of -1 mrad can be compensated by +2 mrad tracking bias, which results into an effective slope error with a mean of 0 mrad. Thus, a similar strategy with tracking correction is applied to each collector samples with exactly twice the mean value of the measured slope error. It is assumed that the tracking correction method is able to reduce the mean value of slope error for any collector to be less than 1 mrad. When such a tracking correction mechanism is applied, the average intercept factor can be improved to 0.991. Tracking correction strategy also makes a great improvement on the IAM curve, as shown in Figure 4.

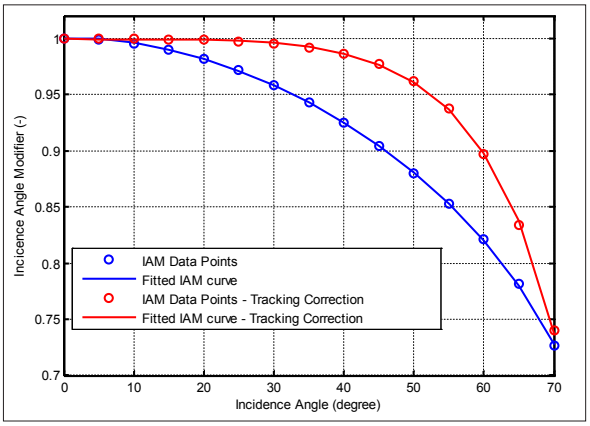

Figure 4. Incidence angle modifier curve: circles mark the predicted data points and the line indicates the fitting function.

Solar Field Model Description

The annual performance of the solar field array at Stillwater was simulated with the Physical Trough model within SAM. The 24,778 m^2 array consists of 11 loops, each loop having two 8-module solar collector assemblies (SCAs) and two 6-module SCAs. The shorter, 6-module SCAs were necessary to allow the trough loops to fit within the available land area. An initial SAM case was created based on the known dimensions of the solar array plus parameters from SkyFuel (collector) and Huiyin (receiver) vendor literature where available. SkyTrough parameters are provided within the SAM Solar Collector library. Default SAM values were used where vendor values were not available. The simulation used pressurized water as the solar-field heat transfer fluid (HTF) for the system. The initial analysis was performed with satellite-

Table 2. Revised input parameters and annual energy output based on measured values at Stillwater.

SAM input parameter	Original case based on SAM default or vendor literature values	Worst case based on measurements at Stillwater in the absence of a tracking offset	Best case based on measurement at Stillwater with Tracking Offset Algorithm
Absorber absorptance (receiver)	0.963	0.96	0.96
Envelope transmittance (receiver)	0.964	0.97	0.97
Mirror reflectance	0.93	0.904	0.904
Geometry effects	0.952	0.883	0.991
Tracking error	0.988	1*	1*
IAM coef. $k_{IAM,0}$	1	1	1
IAM coef. $k_{IAM,1}$	0.0327	0.0138	-0.0140
IAM coef. $k_{IAM,2}$	-0.1351	-0.2234	0.0622
IAM coef. $k_{IAM,3}$	-	0.1225	-0.0909
SAM annual performance prediction for 11-loop, 24,778 m^2 solar field			
Field thermal power produced (MWh/yr)	38,900	35,500	40,700

* tracking error corrections are included in geometry effects

generated solar resource data for Stillwater, NV, for 2013. The site now maintains a pyroheliometer for measurement of direct normal insolation (DNI) that will provide resource data measurements for subsequent simulations.

Following the collector field optical measurements, two cases were created that bound the anticipated field performance based on the effectiveness of the vendor's tracking offset algorithm. Actual performance will be evaluated by on-sun thermal tests. An estimate of solar field thermal energy over the course of a year is given in Figure 5.

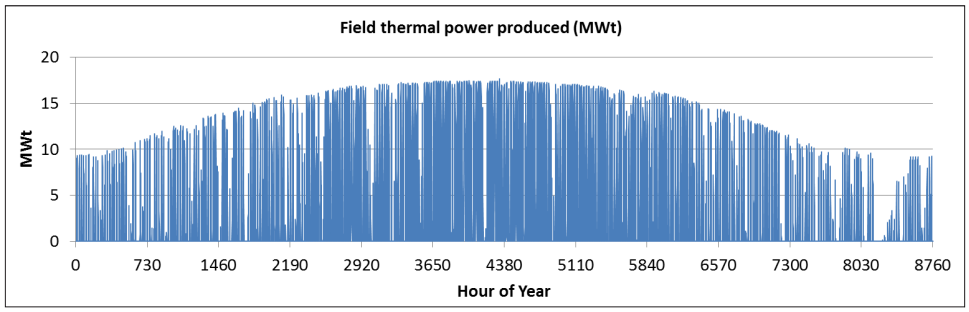

Figure 5. Hourly SAM-predicted solar field thermal energy output for Stillwater based on measured parameters listed in Table 2 and Stillwater, NV, solar resource for 2013.

As noted above, this work found that a third-order IAM equation was required to accurately represent the measured results. This necessitated a revision within SAM, and an internal-NREL version, designated SAM-2015-03-12, was utilized to allow a third-order IAM equation for the analysis. This feature will be available in the next public release of SAM.

The comparison outlined in Table 2 estimates the actual solar field performance will be about 9% lower than the published vendor estimates in the absence of any tracking correction. The greatest deviations are in the mirror reflectance (-3%) and the geometric accuracy of the collector (-7%). It is estimated that a significant boost in performance can be obtained through the tracking correction listed in the previous section. In the correction were 100% effective, this tracking correction could boost the annual field thermal power produced from the un-adjusted level by almost 15%, from 35,500 MWh to 40,700 MWh as shown in Table 2.

Hybrid Plant Model Description

The Stillwater power plant performance was simulated using Aspen Plus V7.3 models developed at the Idaho National Laboratory. Equipment specifications for the major process components were provided by Enel Green Power. The Stillwater power plant utilizes turbines with variable position inlet guide vanes (IGV), variable speed working fluid pumps, and variable speed air-cooled condenser fans. Each of these equipment components is present as multiple items operated in parallel. Certain operating conditions favor curtailing operations from one or more of the parallel equipment components, i.e. during periods of very low ambient temperature one of the cooling fans on each ACC bundle may be operated at a reduced speed or completely powered off.

As described in the previous section, the Stillwater concentrating solar array performance was simulated using the NREL System Advisor Model (SAM). The SAM solar array thermal output was used to compute the heat input to the brine en route to the power plant. This approach allowed the hybrid plant performance to be 'mapped' as a function of brine flow rate (m_{gf}), brine temperature (T_{gf}), solar field thermal output (Q_{solar}), and ambient temperature (T_{air}). Power plant performance was simulated at 576 distinct operating points (unique combinations of four m_{gf}, three T_{gf}, four Q_{solar}, and twelve T_{air} input variable values) and a multidimensional interpolation MATLAB function was utilized to predict performance at intermediate combinations of input variables.

The hybrid plant model was validated using operating data from the Stillwater plant. Net power generation is the primary value of interest for evaluation of hybrid plant performance. Therefore, the model validation evaluated the accuracy of predicted net power generation relative to actual net power generation.

Model validation was performed for both the base and hybrid plant configurations. Several years of base plant operating data was made available by Enel Green Power for validation of the base plant model. Base plant hourly operating data from 2013 was used for model validation purposes. The 2013 Stillwater operating data was parsed to identify week-long (168 hr) periods where the plant operated with a constant number of turbines and without any large disruptions in brine flow rate or temperature due to changes in well field operations. Twelve 168 hr periods meeting these criteria were identified. Ambient temperature values included in these periods ranged from 16°F to 106°F.

The base power plant performance predictions were compared with the plant operating data from each of the twelve 168 hour periods. A coefficient of determination, or R^2, was calculated to evaluate how well the model predictions fit the operational data. The R^2 values for the twelve 168 hr periods evaluated ranged from 0.953 to 0.987, implying very good correlation between predicted and actual values. Additionally, the cumulative power generation predicted by the model was compared with that from the actual plant operations for each of the 168 hr periods. The percentage error was then

calculated to indicate how much the predicted power generation differed from the values obtained from plant operating data. The predicted cumulative power generation for each of the 168 hr periods was within ±2% of the values obtained from plant operating data. This metric provides a useful measure of the model accuracy, since the evaluation of various hybrid plant operating strategies and configurations will require comparison of cumulative power generation over specified time periods. A graphical comparison of the predicted and actual base plant net power generation is provided in Figure 6. Net power generation y-axis values are not provided due to the proprietary nature of the plant operating data.

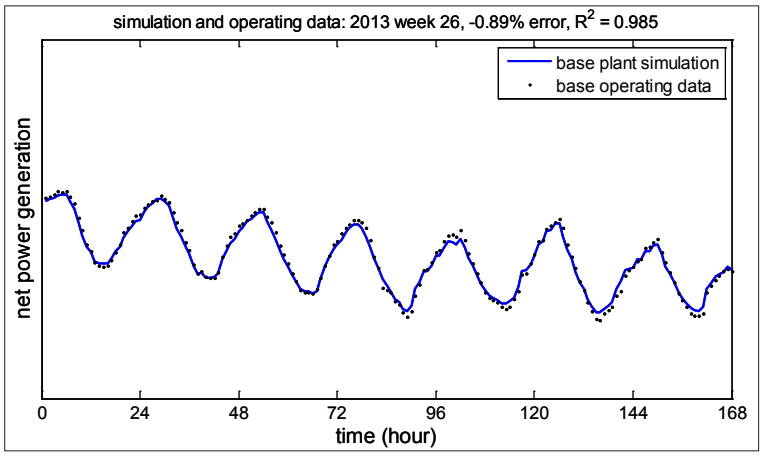

Figure 6. Comparison of simulated and reported base plant net power generation.

A less extensive operating data set was available for validating the hybrid plant model, due to the fact that the Stillwater hybrid plant operations had only recently commenced at the time the model validation was performed. The predicted hybrid plant cumulative power generation was within ±2% of the reported Stillwater hybrid plant power generation with an R^2 value greater than 0.95. Figure 7 is a graphical comparison of the predicted and reported hybrid plant net power generation. The predicted base plant net power generation is included for comparison purposes.

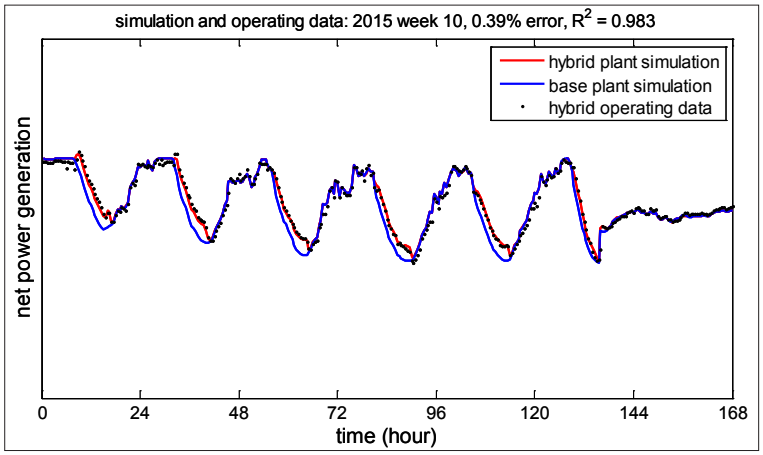

Figure 7. Comparison of simulated and reported hybrid plant net power generation.

Hybrid Plant Optimization

Several Stillwater hybrid plant operating strategies were investigated to identify methods that could be used to optimize hybrid plant performance. This analysis focused on performance optimization of the Stillwater hybrid plant as configured, i.e. the optimization considered modifications to the power plant operations and control strategies but configurations other than the brine preheating were not evaluated. The operating strategies considered include baseline Stillwater hybrid plant operations, IGV position optimization, ACC fan speed optimization, multivariable optimization with control of minimum turbine inlet entropy, and use of mixed working fluids.

The selected power plant operating strategies were evaluated using the validated Aspen Plus Stillwater hybrid plant model with the Aspen Plus Optimization Model Analysis Tool. The operating strategy optimizations sought to maximize net power generation while simultaneously satisfying all plant operating constraints. Operating constraints include specific limits on the working fluid minimum turbine inlet superheat (to prevent expansion within the two-phase region) and geothermal brine minimum exit temperature (to minimize preheater fouling from precipitation of minerals in the geothermal brine). The optimization was constrained to operating points attainable with the existing process operating equipment, i.e. combinations of turbine vane position, control valve position, working fluid pump speed, and ACC fan speed that can be achieved with the existing process equipment.

Plant performance comparisons were made for two operating periods: (1) a one month period representative of March 2015 and (2) a one year period with ambient conditions representative of a typical meteorological year and brine conditions representative of March 2015. The one month period analysis utilized brine temperature, brine flow rate, ambient temperature, and solar DNI data recorded during March 2015 at the Stillwater plant site. The one year period analysis utilized TMY ambient temperature and DNI data, while the average brine flow rate and brine temperature from March 2015 plant operations were used. The baseline hybrid plant turbine IGV position was input using either plant operating data (one month analysis) or a generalized correlation for turbine IGV position based on plant operating data (one year analysis). The number of turbines in service was based on plant operating data for the one month baseline hybrid plant evaluation, while all other evaluations used the configuration that maximized plant performance for each five day interval within the overall analysis period.

Turbine IGV Position Optimization

The Stillwater power block turbines are equipped with adjustable inlet guide vanes (IGVs). The IGV position can be utilized to adjust the turbine inlet pressure and working fluid flow rate. Active IGV control could be utilized to increase plant net power generation and/or respond to short term variances in the hybrid heat sources such as rapid increase or decrease in solar thermal energy input as a result of passing cloud cover.

The Stillwater plant IGVs are manually adjusted by the plant operators to accommodate changes to plant operations (i.e. changes in number of turbines operating or changes in production fluid conditions). The Stillwater IGVs are not typically adjusted in response to changes in ambient temperature.

The baseline hybrid plant simulation was performed using the IGV position reported in the operating data. The effect of optimizing the IGV position, and therefore the working fluid flow rate and turbine inlet pressure, was investigated by allowing the IGV position to be varied in the hybrid plant optimization simulations. It was determined that decreasing the IGV flow area at higher ambient temperatures resulted in decreased working fluid flow rate and increased turbine inlet pressure and temperature, which resulted in greater net power generation. The operating conditions associated with reduced IGV flow area were also utilized at low ambient temperatures to assist in preventing the geothermal brine minimum exit temperature limit from being exceeded. Relative to the baseline Stillwater hybrid plant operation, the hybrid plant model predicts that turbine IGV position optimization would increase net power generation by 1.2% for the March 2015 operating period and 2.0% for the TMY operating period. The optimized IGV position is plotted in Figure 8 as a function of ambient temperature, plant configuration (single and dual turbine operations), and solar heat input for brine conditions representative of March 2015.

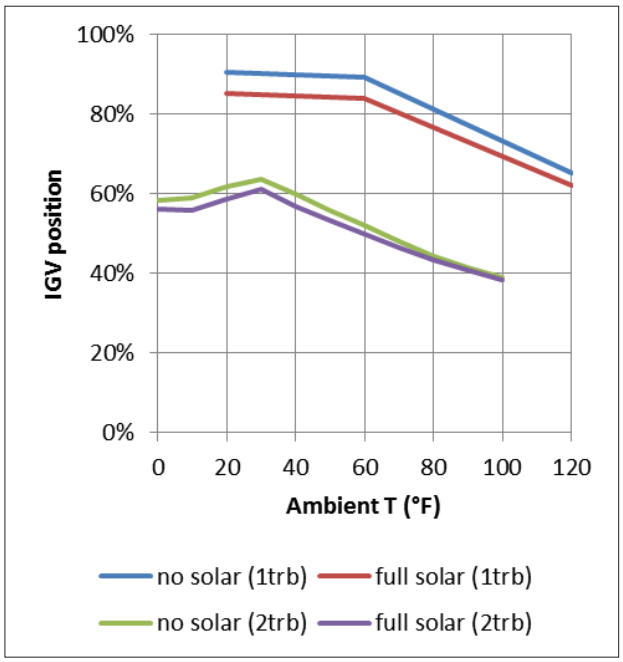

Figure 8. Simulation IGV position as function of ambient temperature, plant operating configuration, and solar heat input (March 2015 brine conditions).

ACC Fan Speed and Turbine IGV Position Optimization

The Stillwater hybrid plant VFD air-cooled condenser fans are slowed during periods of low ambient temperature to reduce power cycle parasitic loads. Reducing the ACC fan speed also assists in preventing working fluid condensation at pressures (and consequently temperatures) that result in the cooling of the geothermal brine to temperatures below the designated temperature limit for prevention of preheater fouling.

The baseline plant simulation used a control strategy that reduced the fan speed at low ambient temperature to prevent the working fluid condensing pressure and the geothermal brine exit temperature from dropping below the designated minimum values. The optimized fan speed simulations eliminated the working fluid condensing pressure constraint and allowed the fan speed to be varied as needed to reduce parasitic loads and maximize net power. When combined with turbine IGV position optimization, the fan speed can be reduced over a wider range of ambient temperature conditions to decrease parasitic loads and increase net power generation. The Stillwater hybrid plant model predicts that combined optimization of ACC fan speed and turbine IGV position would increase net power generation by 1.7% for the March 2015 operating period and 2.9% for the TMY operating period, relative to the baseline hybrid plant

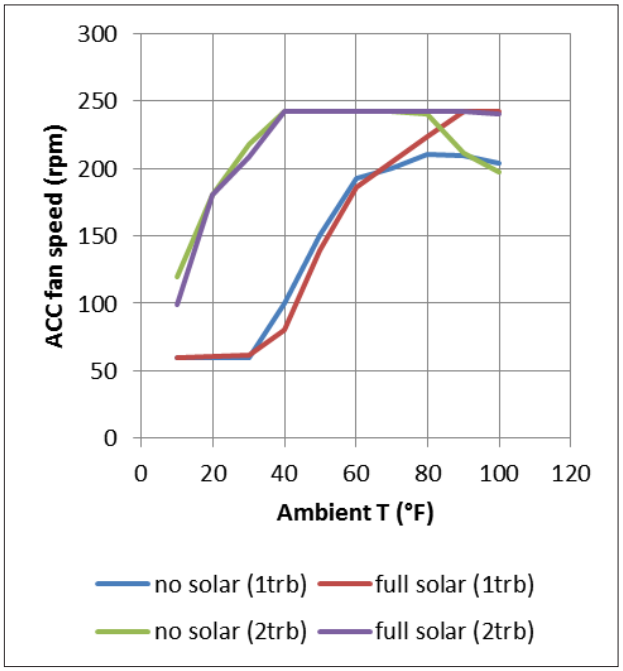

Figure 9. Optimized ACC fan speed as function of ambient temperature, plant operating configuration, and solar heat input (March 2015 brine conditions).

operation. The optimal ACC fan speed is plotted in Figure 9 for various ambient temperatures, plant operating configurations, and solar heat input levels. The geothermal brine minimum exit temperature constraint continued to be satisfied through manipulation of all available process operating variables (ACC fan speed, turbine vane position, control valve position, working fluid pump speed).

Multivariable Optimization Control Strategy

A control strategy that manipulated multiple process variables to control the minimum turbine inlet entropy and maximize net power generation was investigated. The process variables manipulated by this control strategy include the turbine IGV position, ACC fan speed, and working fluid pump speed. The control valve is left in the fully open position with minimal differential pressure drop unless throttling is necessary to satisfy the process operating constraints. In actual operations it is more common for a single process control variable to be associated with a single process operating target; this control strategy may therefore be more complex to implement in an operations environment.

The minimum turbine inlet entropy is a function of temperature and pressure as illustrated in Figure 10. The maximum working fluid dew point entropy is identified as point 'Smax' on the temperature-entropy diagram. At pressures above the maximum dew point entropy pressure, the control strategy adjusts the turbine inlet entropy to the value that corresponds to 1 degree of superheating of the conditions where the maximum dew point entropy occurs. At pressures below the maximum dew point entropy pressure, the control strategy adjusts the turbine inlet entropy to a value that corresponds to 1 degree of superheating. This control strategy prevents turbine inlet conditions that could result in expansion within the two-phase region while minimizing working fluid superheating to increase gross turbine power generation.

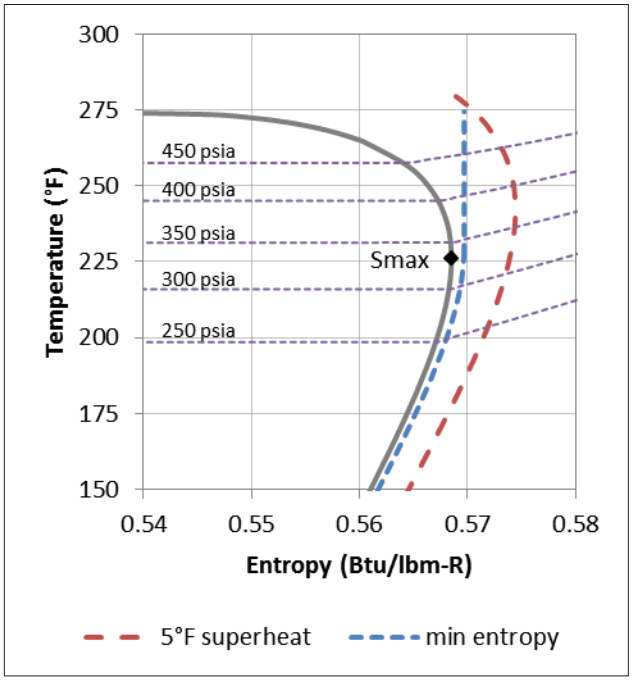

Figure 10. T-S diagram with comparison of minimum entropy vs. constant superheat turbine inlet conditions.

The Stillwater hybrid plant model predicts that the multivariable optimization control strategy would increase net power generation by 2.5% for the March 2015 operating period and 3.8% for the TMY operating period, relative to the baseline hybrid plant operation.

Mixed Working Fluid Retrofit

Mixed working fluids have non-isothermal vaporization and condensation behavior that cause them to perform differently than pure working fluids in organic Rankine cycle operation. The non-isothermal phase change properties of mixed working fluids can eliminate heat exchanger pinch points and decrease the mean temperature difference between the hot and cold fluids so as to reduce power cycle thermodynamic losses. These performance gains typically come at the expense of increased heat exchanger area due to decreased heat transfer performance and heat exchanger mean temperature differences. The potential performance gains associated with mixed working fluids may therefore be negated by the additional capital costs necessary to achieve optimal mixed working fluid power cycle performance.

In the event an organic Rankine cycle is operating at conditions different from the original design conditions, use of mixed working fluids could increase plant performance. The primary power plant equipment requirements include heat exchangers with sufficient heat transfer surface area, multi-pass air-cooled condensers to approximate counter-current condensation, and counter-flow shell and tube style (rather than kettle-type) vaporizers.

The performance of the Stillwater hybrid plant with the multivariable optimization control strategy was evaluated with a 30 wt% propane 70 wt% isobutane mixed working fluid composition. The Stillwater hybrid plant model predicts that the mixed working fluid substitution would increase net power generation by 10.0% for the March 2015 operating period and 7.6% for the TMY operating period, relative to the baseline hybrid plant operation. The evaluation did not consider the detrimental effects of the mixed working fluid on the convective heat transfer coefficients or the possibility of differential condensation (vapor and liquid phases are separated in condenser with a subsequent departure from phase equilibrium conditions) as the current model configuration does not include these capabilities, nor has it been validated for

use with mixed working fluids. The mixed working fluid performance results therefore represent the best case scenario, and further investigation is needed to refine the mixed working fluid results.

Table 3 summarizes the net power generation change of the hybrid plant operating strategies evaluated relative to the baseline Stillwater hybrid plant operation.

Table 3. Predicted net power generation changes for selected hybrid plant optimization strategies relative to baseline Stillwater hybrid plant operation.

	March 2015 power generation	**TMY annual power generation**
input data	**March 2015 Stillwater hybrid plant operating data (ambient T, solar DNI, brine flow, brine T)**	**TMY ambient T and solar DNI; March 2015 Stillwater hybrid plant average brine conditions**
turbine IGV position optimization	+1.2%	+2.0%
ACC fan speed + turbine IGV position optimization	+1.7%	+2.9%
multivariable optimization control strategy	+2.5%	+3.8%
mixed working fluid (30% C_3 + 70% iC_4)*	+10.0%	+7.6%

*effect of mixed working fluid composition on heat transfer coefficients and possibility of differential condensation not considered

Conclusion

CRADA activities have resulted in the optical characterization of the Stillwater hybrid plant solar field and the development and validation of a hybrid plant model. The solar field optical characterization analysis indicated that solar field tracking correction to counteract the effects of reflector slope error and receiver position error could improve the solar field thermal performance by up to 15% relative to uncorrected solar field operation. The hybrid plant model was used to evaluate operating strategies that included turbine IGV position optimization, ACC fan speed and turbine IGV position optimization, turbine inlet entropy control using optimization of multiple process variables, and mixed working fluid substitution. For a one month period with brine and ambient conditions corresponding to March 2015, the hybrid plant model predicted that these operating strategies could result in net power generation increases of up to 10%. For a one year period with brine conditions corresponding to March 2015 and ambient conditions corresponding to a typical meteorological year, the hybrid plant model predicted that these operating strategies could result in net power generation increases of up to 7.6%.

Acronyms

ACC	air-cooled condenser
CRADA	cooperative research and development agreement
CSP/CST	concentrating solar power/thermal
DNI	direct normal insolation
DO	distant observer
EGP	Enel Green Power
GTO	Geothermal Technologies Office
HTF	heat transfer fluid
IAM	incident angle modifier
IGV	inlet guide vanes
INL	Idaho National Laboratory
NREL	National Renewable Energy Laboratory
ORC	organic Rankine cycle
PV	photovoltaic
SAM	System Advisor Model
SCA	solar collector assembly
TMY	typical meteorological year
VFD	variable frequency drive

Acknowledgement

This work was supported by the United States Department of Energy under contract numbers DE-AC07-05ID14517 with the Idaho National Laboratory and DE-AC36-08-GO28308 with the National Renewable Energy Laboratory.

References

1. Astolfi, M., et al., *Technical and economical analysis of a solar–geothermal hybrid plant based on an Organic Rankine Cycle.* Geothermics, 2011. 40(1): p. 58-68.
2. Greenhut, A.D., *Modeling And Analysis Of Hybrid Geothermal-Solar Thermal Energy Conversion Systems*, in *Department of Mechanical Engineering*. 2010, Massachussetts Institute of Technology.
3. Greenhut, A.D., et al. *Solar-Geothermal Hybrid Cycle Analysis For Low Enthalpy Solar And Geothermal Resources*. in *Proceedings World Geothermal Congress*. 2010. Bali, Indonesia.
4. Handal, S., Y. Alvarenga, and M. Recinos. *Geothermal steam production by solar energy*. in *GRC Transactions*. 2007.
5. Lentz, Á. and R. Almanza, *Parabolic troughs to increase the geothermal wells flow enthalpy.* Solar Energy, 2006. 80(10): p. 1290-1295.
6. Lentz, Á. and R. Almanza, *Solar–geothermal hybrid system.* Applied Thermal Engineering, 2006. 26(14-15): p. 1537-1544.
7. Manente, G., *Analysis and Development of Innovative Binary Cycle Power Plants for Geothermal and Combined Geo-Solar Thermal Resources*. 2011, Università degli Studi di Padova.
8. Manente, G., et al. *Hybrid Solar-Geothermal Power Generation To Increase The Energy Production From A Binary Geothermal Plant*. in *Proceedings of the ASME 2011 International Mechanical Engineering Congress & Exposition*. 2011. Denver, Colorado.
9. Paci, M., I. Fastelli, and N. Rossi, *Advanced Systems For Power Production From Geothermal Low Temperature Resources*. 2009.
10. Todorovic, M.S., *Parametric Analysis And Thermodynamic Limits Of Solar Assisted Geothermal Co- And Tri-Generation Systems.* ASHRAE Transactions, 2011.
11. Zhou, C., *Figure of merit analysis of a hybrid solar-geothermal power plant.* Engineering, 2013. 05(01): p. 26-31.
12. Zhou, C., E. Doroodchi, and B. Moghtaderi, *An in-depth assessment of hybrid solar–geothermal power generation.* Energy Conversion and Management, 2013. 74: p. 88-101.
13. Devices & Services Co.; Available from: http://www.devicesandservices.com.
14. Surface Optics Corporation. Available from: http://www.surfaceoptics.com.
15. Stynes, K. and B. Ihas, *Slope Error Measurement Tool for Solar Parabolic Through Collectors*, in *the World Renewable Energy Forum*. 2012: Denver, CO.
16. Stynes, K. and B. Ihas, *Absorber Alignment Measurement Tool for Solar Parabolic Trough Collectors*, in *ASME 2012 6th International Conference on Energy Sustainability*. 2012: San Diego, CA.
17. Zhu, G., et al., *Solar Field Optical Characterization at Stillwater Geothermal/Solar Hybrid Plant.* In preparation, 2015.
18. Zhu, G. and A. Lewandowski, *A New Optical Evaluation Approach for Parabolic Trough Collectors: First-principle OPTical Intercept Calculation (FirstOPTIC).* Journal of Solar Energy Engineering, 2012. 134.
19. NREL. *System Advisor Model 2015.1.30*. Available from: https://sam.nrel.gov/.